New Journal of Physics
The open–access journal for physics

Influence of temperature on the local structure around iodine in fast-ion-conducting AgI:Ag_2MoO_4 glasses

A Sanson[1,3], F Rocca[1], G Dalba[2], P Fornasini[2] and R Grisenti[2]

[1] Istituto di Fotonica e Nanotecnologie del Consiglio Nazionale delle Ricerche Sezione CeFSA di Trento, Via Sommarive 14, I-38050 Povo (Trento), Italy
[2] Dipartimento di Fisica, Universitá degli Studi di Trento, Via Sommarive 14, I-38050 Povo (Trento), Italy
E-mail: andrea.sanson@unitn.it

New Journal of Physics **9** (2007) 88
Received 22 December 2006
Published 11 April 2007
Online at http://www.njp.org/
doi:10.1088/1367-2630/9/4/088

Abstract. Extended x-ray absorption fine structure (EXAFS) measurements have been performed at the K edge of iodine in $(AgI)_{1-y}(Ag_2MoO_4)_y$ glasses, with $y = 0.25$ and 0.33, as a function of temperature from 25 K to the glass transition temperature $T_g \simeq 323$ K. EXAFS monitors the short-range component of the I–Ag distance distribution. At 25 K, iodine coordinates to about four silver ions, at an average distance about 0.06 Å larger than in β-AgI. As temperature increases, EXAFS monitors a progressive depletion of the short-range distribution, due to transitions of Ag ions into a long-range component. Coordination number and mean value of the short-range I–Ag distribution decrease while temperature is increasing. EXAFS results give information on the local modifications around iodine due to the ionic diffusivity.

[3] Author to whom any correspondence should be addressed.

PII: S1367-2630(07)40241-5

Contents

1. Introduction

Fast-ion-conducting (FIC) glasses, whose values of ionic conductivity at room temperature (RT) can be as high as 10^{-2} Ω^{-1} cm^{-1}, are interesting for potential applications in solid state electrochemical devices, such as batteries, smart windows, and sensors, owing to their stability, ease of preparation and large non-stoichiometric compositional ranges [1].

Particular attention has been devoted to FIC glasses containing the doping salt AgI. The continuous experimental progress, based on the use of many experimental techniques, like nuclear magnetic resonance, infra-red and Raman spectroscopies, x-ray absorption fine structure (XAFS), x-rays and neutron diffraction, has led to the development of more and more refined models and to some commonly accepted ideas. However, a definitive satisfactory explanation of ionic conduction has not yet been obtained. A recent review of experimental results and theoretical models for AgI-doped FIC glasses can be found in [2] and references therein.

Silver molybdate glasses, where the doping salt AgI is embedded in a glassy matrix Ag_2O–$M_\alpha O_\beta$ (typically M = B, P, Mo) [3], are particularly important for studying the relationship between structure and transport properties [4]–[11]. Contrary to AgI-doped silver-borate and silver-phosphate glasses, where the binary matrices Ag_2O–B_2O_3 and Ag_2O–P_2O_5 form continuous random networks, AgI-doped silver-molybdate glasses are depolymerized systems, where the oxy-anions, mainly represented by $(MoO_4)^{2-}$ tetrahedra, do not form networks. The glass formation region is limited to a fixed ratio $[Ag_2O]/[MoO_3] = 1$ and to a narrow interval of values of the ratio $y = [Ag_2MoO_4]/([AgI] + [Ag_2MoO_4])$, ranging from about 0.25 to about 0.43. The unusually low glass transition temperature, T_g, lies in the range 310–350 K, depending on composition [8, 12].

According to Mustarelli *et al* [2, 13], the addition of AgI to the modified glassy matrix Ag_2O–MoO_3 causes a progressive increase of the silver ions in mixed coordination state, I–Ag–O, and there is evidence that the mobile Ag^+ cations responsible for ionic conductivity are those which share bonds with both iodine and oxygen atoms.

The aim of the present work is to study the local environment of the iodine anion in the glasses AgI–Ag_2MoO_4 as a function of temperature, by means of extended XAFS (EXAFS). Temperature-dependent structural studies of FIC glasses are important for understanding the conduction mechanism, since the transport properties strongly depend on the temperature. To our knowledge, this kind of study has not yet been performed in these glasses, in spite of their

relevance. Besides, EXAFS is particularly suited to studying the local environment of a given type of atom in multicomponent glasses, owing to its selectivity of atomic species and insensitivity to long-range order [14].

The paper is organized as follows. In section 2, details on sample preparation and EXAFS measurements are given. In section 3, the procedure of data analysis adopted in this work is critically described. In section 4 the results of EXAFS data analysis are presented and discussed. Section 5 is dedicated to conclusions.

2. Experimental

Two glasses $(AgI)_{1-y}(Ag_2MoO_4)_y$, with $y = 0.25$ and 0.33, were prepared by the melt–quenching technique. Appropriate mixtures of AgI (Aldrich 99%) and Ag_2MoO_4 (prepared by precipitation from aqueous solution of $AgNO_3$ and Na_2MoO_4, as in [15]) were melted at 873 K for 2 h in alumina crucibles and then quenched down to RT in air on stainless steel plates [12]. The glass transition temperature, measured by differential scanning calorimetry (DSC), was 323 K for both glasses [12]. The possible presence of crystallites in the glasses was limited to below the detectability threshold of laboratory x-ray diffraction.

EXAFS measurements at the K edge of iodine (33.169 keV) were performed in transmission mode at the beamline BM29 of ESRF in Grenoble (France), equipped with a flat-face Si(311) double crystal monochromator. Storage ring energy and average current were 6.0 GeV and 200 mA, respectively. To get homogeneous samples of uniform thickness, the glasses were powdered, dispersed in alcohol and slowly deposited on polytetrafluoroethylene membranes. The thickness was calibrated in order to obtain an absorption edge jump $\Delta\mu x \simeq 1$ at the K edge of iodine. The samples were maintained in a He atmosphere (200 mbar) to ensure thermal exchange with a cold finger in contact with liquid He flow. The temperature was varied from 25 to T_g utilizing a closed-cycle helium cryostat. Crystalline β-AgI was also measured as reference at low temperatures. The edges of all spectra were aligned to within 0.1 eV or better, in order to obtain a resolution of the order of 0.001 Å in relative distances.

The EXAFS signals $\chi(k)$, where k is the photoelectron wavevector, were extracted from the experimental spectra according to well established procedures [16], and are shown in figure 1 at 25 and 300 K. The quality of EXAFS data is good up to 15 $Å^{-1}$ even at the highest temperature.

3. Data analysis

The $k\chi(k)$ weighted EXAFS signals were Fourier transformed in the interval $k = 2.4$–$15\ Å^{-1}$ using a Gaussian window. The Fourier transforms (imaginary part and modulus) of the EXAFS signals of crystalline β-AgI at 300 K and of the glass $y = 0.25$ at 25 and 300 K are compared in figure 2, while the moduli of the Fourier transforms of both glasses at selected temperatures are shown in figure 3. The structure between about 1.5 and 3 Å is due to the contribution of nearest-neighbours Ag ions, although not all Ag ions necessarily contribute to it. The attribution to Ag ions is supported by the striking similarity of the Fourier transforms of the glasses and β-AgI in the range from 1.5 to 3 Å, and by the results of recent EXAFS measurements at the Mo K edge, which exclude the presence of a nearest-neighbour link between iodine and

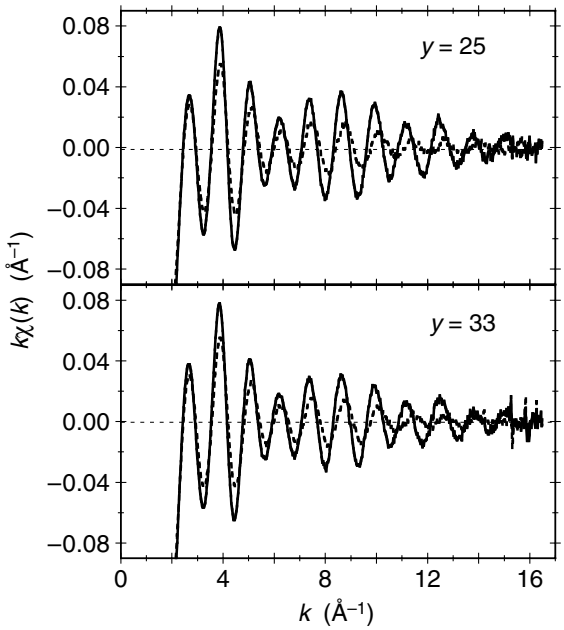

Figure 1. Weighted EXAFS signals $k\chi(k)$ at 25 and 300 K (solid and dashed lines, respectively) for the glass $y = 0.25$ (top panel) and the glass $y = 0.33$ (bottom panel).

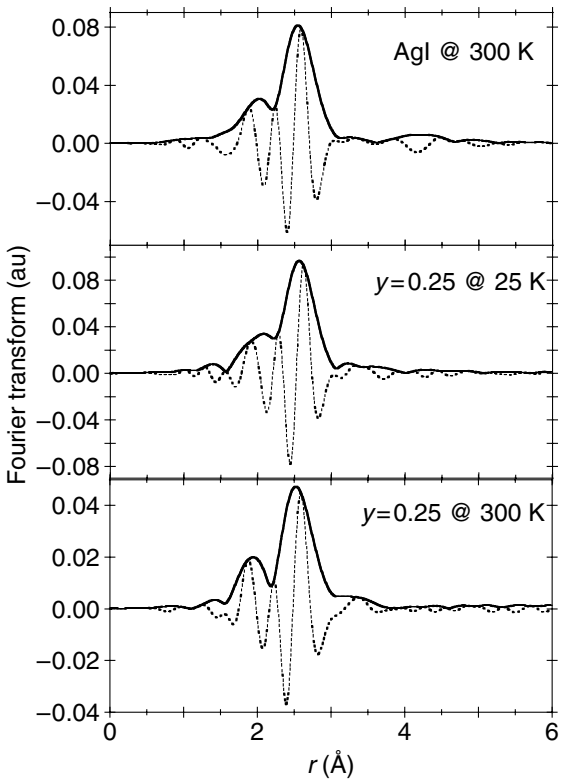

Figure 2. Fourier transforms of the EXAFS signals of β-AgI at 300 K (top panel) and of the glass $y = 0.25$ at 25 and 300 K (middle and bottom panel). Dashed and continuous lines are the imaginary part and the modulus, respectively.

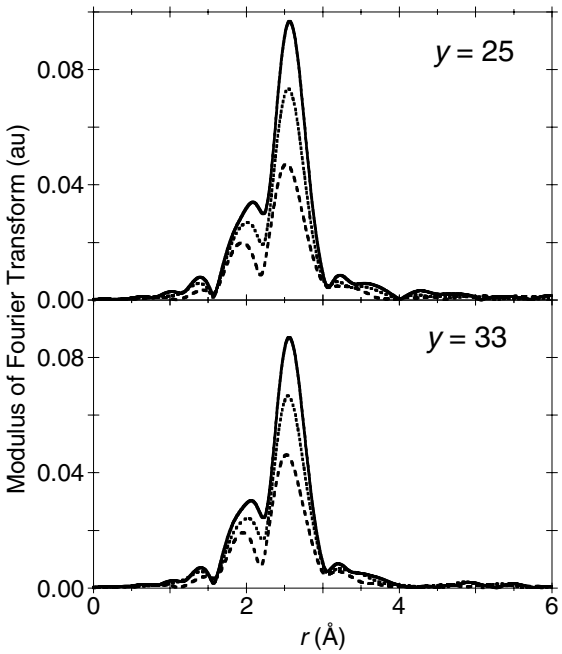

Figure 3. Moduli of Fourier transforms for the glass $y = 0.25$ (top panel) and the glass $y = 0.33$ (bottom panel) at 25 K (continuous line), 150 K (dotted line) and 300 K (dashed line).

molybdenum [17]. A nearest-neighbour link between negative iodine and oxygen ions is highly improbable. No neat contribution from farther neighbours is visible in the Fourier transforms of the glasses even at the lowest temperature, owing to the effect of disorder.

The structure between about 1.5 and 3 Å was Fourier back-transformed, and the filtered EXAFS signal analysed by the *ratio method* using the cumulant approach [18, 19]. Each glass was separately analysed, using its lowest temperature spectrum as reference for backscattering amplitudes, phase shifts and inelastic terms. The low-temperature spectra of the glasses were in turn calibrated against the low-temperature spectrum of β-AgI.

The cumulant analysis allows one to effectively take into account the asymmetry of the distance distribution, which never can be neglected if accurate values of average distances are sought [20, 21]. However, in the case of systems affected by relatively strong structural disorder, as is the case of FIC glasses, the cumulant analysis is in principle questionable [22]. To obtain reliable results, the present work has been based on the following considerations and guidelines.

An EXAFS experiment samples an *effective* distribution of nearest-neighbours distances

$$P(r, k, T) = N\rho^*(r, T) \exp[-2r/\lambda(k)]/r^2, \tag{1}$$

where k is the photoelectron wavevector, N is the coordination number, ρ^* is the *real* distribution and $\lambda(k)$ is the photoelectron mean free path. The cumulants C_n can be defined [18] as the coefficients of the MacLaurin expansion

$$\int_0^\infty P(r, k, T) e^{2ikr}\, dr = \exp\left[\sum_{n=0}^{\infty} (2ik)^n C_n(k, T)/n!\right], \tag{2}$$

and are connected to the cumulants C_n^* of the real distribution by simple analytical relations [19]. First and second cumulants, C_1^* and C_2^*, correspond to the mean and variance of the distribution, respectively, while the higher order cumulants monitor the deviation from a gaussian shape; in particular, the third cumulant measures the asymmetry; C_0^* is proportional to the coordination number. The ratio method consists of separately comparing phases and amplitudes of the EXAFS signals of a sample (s) and a reference (r) and in fitting the difference of phases and logarithm of amplitudes ratio to finite polynomials corresponding to the cumulant series (2) truncated at low order terms. The ratio method thus gives the relative values $\Delta\tilde{C}_n = \tilde{C}_{n,\mathrm{s}} - \tilde{C}_{n,\mathrm{r}}$ of a few polynomial coefficients, as well as the ratio of coordination numbers $N_\mathrm{s}/N_\mathrm{r}$.

The convergence interval of the series in the right-hand side of equation (2) progressively reduces to lower k values when the deviation of the distribution from the normal shape increases. The limits of the cumulant method have been thoroughly studied by Crozier *et al* [23] and by Yang *et al* [24]; these authors have shown that, when the EXAFS signal is analysed within a range extending beyond the convergence interval of the cumulant series, the polynomial coefficients given by the EXAFS analysis do not reproduce the cumulants, and a reduced coordination number is obtained.

In the case of weak thermal disorder, the temperature dependence of the lowest order cumulants is expected to follow a well-defined temperature dependence [25, 26]. The convergence properties of the cumulant series can thus be confirmed by checking the correspondence of the temperature dependence of the polynomial coefficients with that expected for cumulants [16, 20, 21].

In their pioneering study of the superionic phase transition of AgI, Boyce *et al* [27] found a 25% reduction of the I–Ag coordination number in the superionic α phase with respect to the expected value $N = 4$, when they firstly analysed EXAFS by a standard technique. In subsequent more refined works, they obtained a good fit of experimental data to an excluded-volume model, whose asymmetric distribution contains four silver ions, and is characterized by a tail extending to long distances, which represents the conduction pathway [28].

To hypothesize a model distribution is however much more difficult for noncrystalline solids and liquids than for a crystal like α-AgI, where iodine ions form a rigid sublattice. A solution to this problem has been suggested by Filipponi [22]. The basic idea is to separate the nearest-neighbours distribution into a short-range narrow asymmetric distribution and a long-range tail; the long-range tail is independently obtained from other techniques, like diffraction experiments plus reverse Monte Carlo (RMC) modelling, and only the parameters of the short-range distribution are used as fitting parameters in the EXAFS analysis. An application of this procedure has been recently made to CuI, in both superionic and liquid phases [29].

The feasibility of this approach depends on the availability of a reliable long-range tail distribution, which can be difficult to obtain in the case of many-component glasses at various temperatures, as required by our present study. To our knowledge, the only work on AgI-doped silver-molybdate glasses based on diffraction and RMC modelling has been made only at RT, and no partial radial distributions have been published [9]. To overcome this difficulty, a new approach to the cumulant method for superionic glasses has been devised, following the first pioneering idea of Boyce *et al* [27]. The data analysis is extended to the whole available k range, allowing a full exploitation of the high quality of the EXAFS signal, and the polynomial coefficients obtained from the ratio method, instead of being referred to the *whole* effective distribution of nearest-neighbour silver ions, are considered to parametrize a *short-range* narrow component of the whole distribution, corresponding to the Ag ions more tightly bound to iodines; the

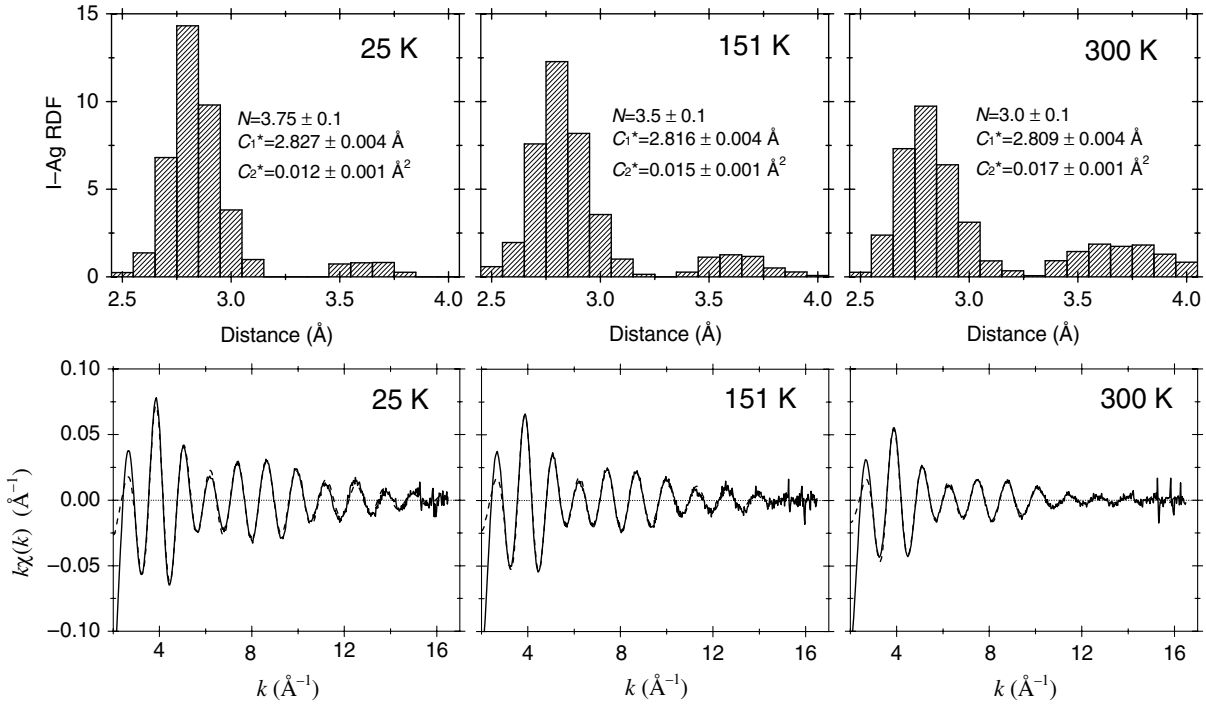

Figure 4. I–Ag distribution at three selected temperatures (top panels) obtained in glass $y = 0.33$ by direct simulations of the experimental EXAFS signals (bottom panels). Experimental and simulated signals are plotted in solid and dashed lines, respectively. Coordination number (i.e. area distribution), mean value and variance of each *short-range* distribution ($r \leqslant 3.2$ Å) are reported in the top panels. The quoted uncertainties do not account for the possible inaccuracy of theoretical backscattering amplitudes and phase-shifts calculated by FEFF8 [30].

remaining long-range tail, which escapes EXAFS detection, contains Ag ions directly related to conduction.

The soundness of this interpretation of EXAFS cumulant as referring to the short-range distribution has been tested as follows. The EXAFS signal was simulated for an arbitrary starting distribution of I–Ag distances and compared with the experimental signal at different temperatures. The distribution was then varied, by means of a Monte Carlo procedure, in order to optimize the agreement between simulated and experimental signals. Independently of the shape of the starting distribution (from narrow to flat), the final distribution was always characterized by two components, one rather sharp and short-ranged, the other rather flat and long-ranged (figure 4). The EXAFS signal due to the long-range component is negligible. When temperature increases, the short-range distribution progressively decreases, while the long-range distribution progressively grows. More importantly, the temperature dependence of the short-range component and its cumulants were in very good agreement with the results of the analysis performed by the ratio method (see below).

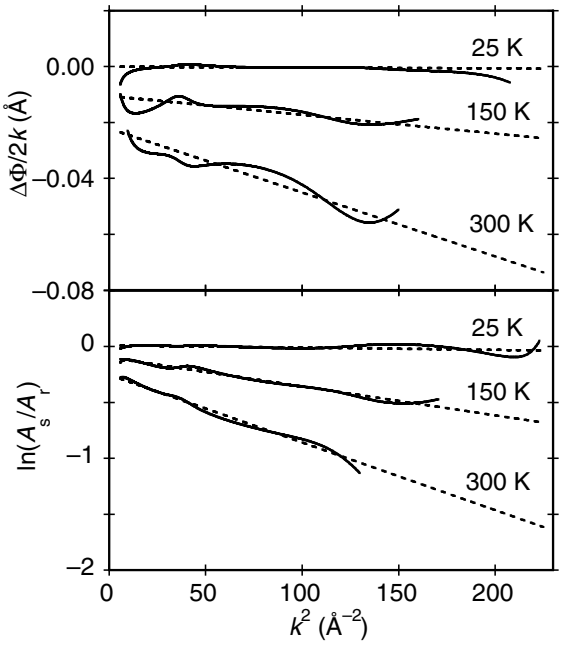

Figure 5. Weighted difference of phases $(\Phi_s - \Phi_r)/2k$ and logarithm of amplitudes ratio $\ln(A_s/A_r)$ for the glass $y = 33$, plotted against k^2 at 25, 150 and 300 K.

4. Results and discussion

The phase differences and the logarithms of amplitude ratios are shown in figure 5 for the $y = 0.33$ molybdate glass at selected temperatures; similar results were obtained for the glass $y = 0.25$. The ratio method completely disentangles amplitude parameters (N and $\tilde{C}_2$) from phase parameters ($\tilde{C}_1$ and $\tilde{C}_3$); besides, the linearity of the fitting procedure allows an easy evaluation of the possible correlation of the pairs of parameters involved in the separate analyses of amplitude and phase, since they are measured by intercept and slope of the best-fitting straight lines, respectively [18]. In this case, significant correlation effects between N and $\tilde{C}_2$ and between $\tilde{C}_1$ and $\tilde{C}_3$ can be excluded simply by visual inspection.

The coordination number N and the first three polynomial coefficients $\tilde{C}_i$ ($i = 1$–3) obtained from the ratio method are shown in figures 6 and 7. The corresponding cumulants of the reference β-AgI, measured at low temperature (current experiment) and in a wider temperature range (previous EXAFS experiment [31]), are also shown. Absolute values of the second polynomial coefficients $\tilde{C}_2$ have been obtained by fitting a correlated Einstein model to the experimental relative values of the second cumulant of β-AgI.

According to the guidelines of section 3, the polynomial coefficients $\tilde{C}_i$ are interpreted as the cumulants of an asymmetric short-range distribution of I–Ag distances. The reliability of this interpretation is given by the good agreement between the cumulants obtained by the ratio method, and the cumulants of the distributions obtained by the independent simulation described at the end of the previous section, whose results for glass $y = 0.33$ are summarized in figure 4. In both procedures, in fact, from 25 to 300 K the mean I–Ag distance shrinks by about 0.02 Å, the coordination number changes from about 3.8 to 3.0, the variance exhibits very similar values.

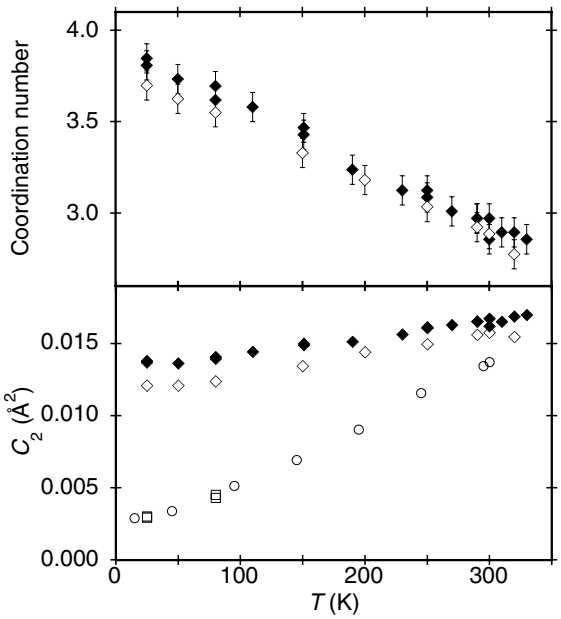

Figure 6. Temperature dependence of coordination number (top panel) and variance (bottom panel) of the short-range distribution of I–Ag distances in glasses $y = 0.25$ (open diamonds) and $y = 0.33$ (full diamonds). Squares and circles refer to β-AgI measured in the current experiment and in the experiment of [31], respectively.

4.1. Low-temperature distributions

Let us first consider the results at the lowest temperature (25 K). The average I–Ag distance measured by EXAFS in the glasses is larger than in β-AgI, by about 0.06 Å in the AgI-poorer glass $y = 0.33$ and by about 0.05 Å in the AgI-richer glass $y = 0.25$ (figure 7, top panel). The coordination number is about 3.8, and can reasonably be extrapolated to 4 at 0 K for the glass $y = 0.33$, but is slightly lower for the glass $y = 0.25$ (figure 6, top panel). The second cumulant of the glasses, measuring the variance of the short-range I–Ag distance distribution, is about five times larger than the zero point value for β-AgI, which is assumed to be of purely thermal origin (figure 6, bottom panel). The difference with respect to β-AgI is larger for the glass $y = 0.33$. Also the third cumulant, measuring the asymmetry of the short-range distribution, is remarkably large, the thermal contribution in β-AgI being comparatively negligible (figure 7, bottom panel).

The low temperature results can be interpreted according to the following picture. Iodine ions in the glasses are surrounded by an average of approximately four silver ions. The distribution of I–Ag distances probed by EXAFS is much wider than in β-AgI (second cumulant); its average value (first cumulant) is about 0.06 Å larger (the difference corresponding to about half the bond distance standard deviation $\sqrt{C_2}$), and the skewness parameter $C_3/C_2^{1.5}$ is about 0.5. This situation is the effect of both site disorder (different inequivalent iodine sites) and local disorder (four different I–Ag distances around each iodine).

In view of the impossibility of evaluating the convergence properties of the cumulant series, one cannot *a priori* establish a quantitative connection between the short-range distribution probed by EXAFS and the whole distribution of I–Ag distances. The convergence defect of the cumulant series of the whole distribution, however, generally induces a reduction of the

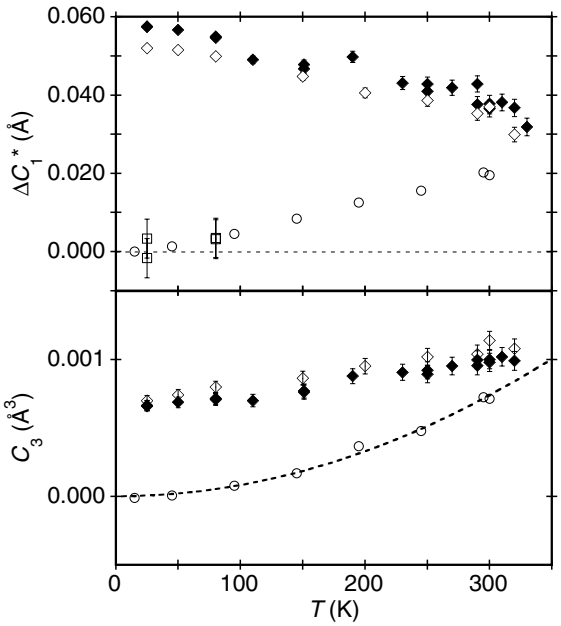

Figure 7. Temperature dependence of the mean value (top panel) and third cumulant (bottom panel) of the short-range distribution of I–Ag distances in glasses $y = 0.25$ (open diamonds) and $y = 0.33$ (full diamonds). Squares and circles refer to β-AgI measured in the current experiment and in the experiment of [31], respectively.

coordination number and of the polynomial coefficients with respect to the cumulants [23, 24]. If one assumes the tendency of iodine atoms to coordinate four silver atoms, the fact that $N \to 4$ for $T \to 0$ suggests that at very low temperatures the reduction is not dramatic, and the short-range distribution probed by EXAFS is a good approximation of the whole distribution, in particular for the glass $y = 0.33$. This consideration is in agreement with the simulated distribution at 25 K displayed in the first panel of figure 4.

If the effect of thermal disorder is similar for all nearest-neighbour atomic pairs, the short-range distribution of distances is the convolution of two distributions, due to structural and thermal disorder, respectively; in this case, the EXAFS cumulants are the sum of two terms, one thermal and one structural [18]. The effects of vibrational motion on the EXAFS signals of nearest-neighbour pairs are generally quite insensitive to long-range order [32], so that they can be assumed similar for all I–Ag nearest-neighbour atomic pairs in glasses and in β-AgI; the differences between second and third cumulants in glasses and β-AgI at low temperature, $\Delta C_2^{\mathrm{str}} \simeq 0.01$ Å^2 and $\Delta C_3^{\mathrm{str}} \simeq 0.0007$ Å^3, are thus a rough measure of the effects of structural disorder. A simple Monte Carlo test shows that these cumulant values are consistent with one longer and three shorter I–Ag distances, differing by about 0.2 Å. It is reasonable to assume that the longer I–Ag distance concerns Ag ions bridging between iodine ions and $(MoO_4)^{2-}$ molybdate units.

Actually, the AgI-poorer glass $y = 0.33$, which has a larger number of Ag–O bonds than the glass $y = 0.25$, exhibits a larger difference of mean and width of the distribution with respect to β-AgI. On the other hand, the lower value of coordination number in the AgI-richer glass $y = 0.25$ could be attributed to the presence of a non-negligible long-range distribution, escaping EXAFS

detection, already at low temperatures. The transfer of Ag ions from the short-range distribution to the long-range tail probed by EXAFS can be connected to the mechanism of ionic conductivity. Actually, the glass $y = 0.25$ is characterized by a dc ionic conductivity about one order of magnitude higher than the glass $y = 0.33$ [8].

4.2. Dependence on temperature

The temperature dependence of the EXAFS cumulants monitors relative variations of the local structure, and its interpretation is to a good extent independent of the quantitative accuracy of absolute values referring to the low temperature model depicted in the previous subsection.

It is evident from figure 6 (top panel) that the coordination numbers are reduced from $N \simeq 4$, at 0 K, to about 3, at 300 K. This reduction can be considered as due to the progressive breakdown of the convergence of the cumulant series of the *whole* distribution [23, 24]. However the value N obtained from the ratio method is a measure of the number of Ag ions populating the short-range distribution probed by EXAFS, and the reduction of N with temperature is due to the progressive transfer of silver ions from the short-range distribution to a long-range tail that escapes EXAFS detection.

Let us now consider the temperature dependence of the first three polynomial coefficients $\tilde{C}_i$. When temperature increases up to T_g, the average I–Ag distance measured by EXAFS decreases by more than 0.02 Å in both glasses (figure 7, top panel); this behaviour is compared with the expansion of the I–Ag average distance in β-AgI in the same temperature range. The nearest-neighbours thermal expansion measured by EXAFS is always greater than the expansion measured by Bragg diffraction (in crystals) or by dilatometric techniques, owing to the effect of perpendicular atomic vibrations [19]. The reduction of the average I–Ag distance measured by EXAFS in the glasses cannot be attributed to a bond contraction of purely thermal origin, since this interpretation would be inconsistent with the positive macroscopic expansion measured by dilatometric techniques [7], as well as with the experimental evidence that the nearest-neighbours distance increases with temperature also in materials with negative macroscopic thermal expansion [33].

The increase with temperature of the width of the I–Ag distribution measured by EXAFS in the glasses is much weaker than that of β-AgI (figure 6, bottom panel). Also the asymmetry of the distribution measured by EXAFS in the glasses has a much weaker increase with temperature than the third cumulant of β-AgI (figure 7, bottom panel). On the basis of experimental results on simpler systems, like amorphous germanium [32], it is reasonable to assume that the effects of local atomic vibrations on the distribution of the nearest-neighbours distances are not very different in amorphous systems and in their crystalline counterparts. The weaker temperature dependence of width and asymmetry of the short-range distributions in glasses, with respect to β-AgI, cannot be reasonably attributed only to a different local vibrational behaviour. A further (negative) contribution on the temperature dependence of width and asymmetry must be given by the progressive migration of the Ag ions from the short-range to the long-range component, as monitored in figure 4.

When temperature increases, the short-range distribution is progressively depleted of silver ions (decrease of N); the ions lost by the short-range distribution populate the long-range distribution, which is reasonably connected with the conduction pathways. The decrease of N measured by EXAFS corresponds to the progressive reduction of the convergence interval of the cumulant series of the whole distribution, and can be physically explained as follows. The Ag ions

in the long-range part give rise to a coherent signal mainly by scattering the long-wavelength photoelectrons (low k values); the short-wavelength photoelectrons (intermediate and high k values), scattered by different regions of the long-range tail, give rise to signals which interfere destructively, and do not contribute to EXAFS. When the population of the long-range tail increases, a larger number of Ag ions escape detection, and the coordination number decreases.

It is reasonable to assume that the silver ions more distant from iodine ions, and then less tightly bound, are more easily transferred from the short-range distribution to the long-range conduction tail. This behaviour clarifies the possible negative contribution to the temperature dependence of width and the asymmetry of the short-range distribution, as well as the reduction of its average value (I–Ag distance). Actually, the percent of Ag ions more tightly bound and closer to iodine would increase with temperature within the short-range distribution. This picture is supported by the slight differences observed for the two measured glasses. The AgI-richer glass $y = 0.25$, characterized by a stronger ionic conductivity at all temperatures, shows systematically lower values of coordination number, average I–Ag distance and width of the distribution with respect to the glass $y = 0.33$.

The EXAFS results could be interpreted also in terms of a more elaborate qualitative picture, according to which the migration of an Ag^+ ion would induce a local structural relaxation of the remaining Ag ions around the involved iodine ion, that would contribute to the reduction of structural disorder. This second picture, rather than alternative to the previous one, should be considered more complete. Anyway, to the extent that the Ag ions more distant from iodine are those bridging between iodine and molybdate units, our interpretation of EXAFS results in terms of progressive depletion of the short-range distribution by the Ag ions more distant from iodine strongly supports some recent models, according to which the pathways for ionic conduction are characterized by mixed iodine–oxygen environments [2].

If the I–Ag long-range component of the whole distance distribution is entirely due to the Ag ions in diffusion, the ratio $N/4$, where N is the coordination number measured by EXAFS, can be considered an estimate of the ratio $\tau_d/(\tau_d + \tau_f)$, where τ_d and τ_f are the dwelling and flight times of Ag ions, respectively. The value $\tau_d/(\tau_d + \tau_f) \simeq 0.7$ found in this work at 300 K for molybdate glasses is comparable with the value 0.75 found by Boyce *et al* [27] in their first study of α-AgI. The difference in dc conductivity, which in α-AgI at 420 K is much higher than in molybdate glasses near T_g (about 1 Ω^{-1} cm^{-1} and 10^{-2} Ω^{-1} cm^{-1}, respectively) is not due to a different ratio between dwelling and flight times, but to a very different jump frequency, which is inversely proportional to the sum $\tau_d + \tau_f$.

5. Conclusions

EXAFS at the iodine K edge has been measured as a function of temperature in two AgI-doped silver-molybdate glasses with different compositions. In spite of the large structural disorder, an analysis based on the cumulant method has been made possible by referring the experimental cumulants not to the whole distribution of I–Ag distances, but only to its short-range component. The long-range contribution connected to ion conduction escapes EXAFS detection.

The temperature dependence of EXAFS cumulants gives original insights into the behaviour of the local environment of iodine, as a result of the increase of the Ag ions diffusion: coordination number and average value of the short-range distribution decrease when temperature increases, while width and asymmetry of the distribution increase much less than expected in terms of purely

vibrational disorder. These results are interpreted as monitoring the progressive transition of Ag ions from the short-range distribution to the long-range conduction tail, and are consistent with the models of conduction based on pathways characterized by mixed iodine–oxygen environments.

Acknowledgments

We acknowledge C Armellini for help in sample preparation, ESRF for provision of synchrotron radiation and S De Panfilis and the staff of the ESRF-BM29 beamline for experimental assistance. This work has been partially supported by the ESRF project HS-2463. AS acknowledges the support of the Provincia Autonoma di Trento, through the LOTHEX project at IFN-CNR.

References

[1] Vashista P, Mundy J N and Shenoy G K 1979 *Fast Ion Transport in Solids* (New York: Elsevier)
[2] Mustarelli P, Tomasi C and Magistris A 2005 *J. Phys. Chem.* B **109** 17417
[3] Magistris A 1993 *Fast Ion Transport in Solids* ed B Scrosati *et al* (Dordrecht: Kluwer) pp 213–30
[4] Minami T, Katsuda T and Tanaka M 1978 *J. Non-Cryst. Solids* **29** 389
[5] Minami T and Tanaka M 1980 *J. Non-Cryst. Solids* **38–39** 289
[6] Minami T and Tanaka M 1980 *J. Non-Cryst. Solids* **42** 469
[7] Almond D P, Duncan G K and West A R 1985 *J. Non-Cryst. Solids* **74** 285
[8] Kawamura J and Shimoji M 1986 *J. Non-Cryst. Solids* **88** 281
[9] Swenson J, McGreevy R L, Börjesson L, Wiks J D and Howells W S 1996 *J. Phys.: Condens. Matter* **8** 3545
[10] Mustarelli P, Tomasi C, Quartarone E, Magistris A, Cutroni M and Mandanici A 1998 *Phys. Rev.* B **58** 9054
[11] Bhattacharya S and Ghosh A 2005 *J. Phys.: Condens. Matter* **17** 5655
[12] Tomasi C, Mustarelli P and Magistris A 1998 *J. Solid State Chem.* **91** 140
[13] Mustarelli P, Tomasi C, Magistris A and Cutroni M 1998 *J. Non-Cryst. Solids* **232–234** 532
[14] Hayes T M and Boyce J B 1982 *Solid State Phys.* **37** 173
[15] Kohlmuller R and Faurie J P 1968 *Bull. Soc. Chim. Fr.* **11** 4379
[16] Dalba G, Fornasini P and Rocca F 1993 *Phys. Rev.* B **47** 8502
[17] Rocca F, Kuzmin A, Mustarelli P, Tomasi C and Magistris A 1999 *Solid State Ionics* **121** 189
[18] Bunker G 1983 *Nucl. Instrum. Methods Phys. Res.* **207** 437
[19] Fornasini P, Monti F and Sanson A 2001 *J. Synchrotron Radiat.* **8** 1214
[20] Fornasini P, a Beccara S, Dalba G, Grisenti R, Sanson A, Vaccari M and Rocca F 2004 *Phys. Rev.* B **70** 174301
[21] Dalba G, Fornasini P, Grisenti R and Purans J 1999 *Phys. Rev. Lett.* **82** 4240
[22] Filipponi A 2001 *J. Phys.: Condens. Matter* **13** R23–R60
[23] Crozier E D, Rehr J J and Ingalls R 1988 *X-ray Absorption* ed D C Koningsberger and R Prins (New York: Wiley) chapter 9, pp 373–442
[24] Yang D S, Fazzini D R, Morrison T I, Tröger L and Bunker G 1997 *J. Non-Cryst. Solids* **210** 275
[25] Frenkel A I and Rehr J J 1993 *Phys. Rev.* B **48** 585
[26] Yokoyama T 1999 *J. Synchrotron Radiat.* **6** 323
[27] Boyce J B, Hayes T M, Stutius W and Mikkelsen J C Jr 1977 *Phys. Rev. Lett.* **38** 1362
[28] Boyce J B, Hayes T M and Mikkelsen J C Jr 1981 *Phys. Rev.* B **23** 2876
[29] Trapananti A, Di Cicco A and Minicucci M 2002 *Phys. Rev.* B **66** 014202
[30] Ankudinov A, Ravel B, Rehr J and Conradson S 1998 *Phys. Rev.* B **58** 7565
[31] Dalba G, Fornasini P, Rocca F and Monti F 2001 *J. Non-Cryst. Solids* **293–295** 93
[32] Dalba G, Fornasini P, Grazioli M and Rocca F 1995 *Phys. Rev.* B **52** 11034
[33] Sanson A, Rocca F, Dalba G, Fornasini P, Grisenti R, Dapiaggi M and Artioli G 2006 *Phys. Rev.* B **73** 214305